SUPPLEMENTAL INFORMATION

Figure S1

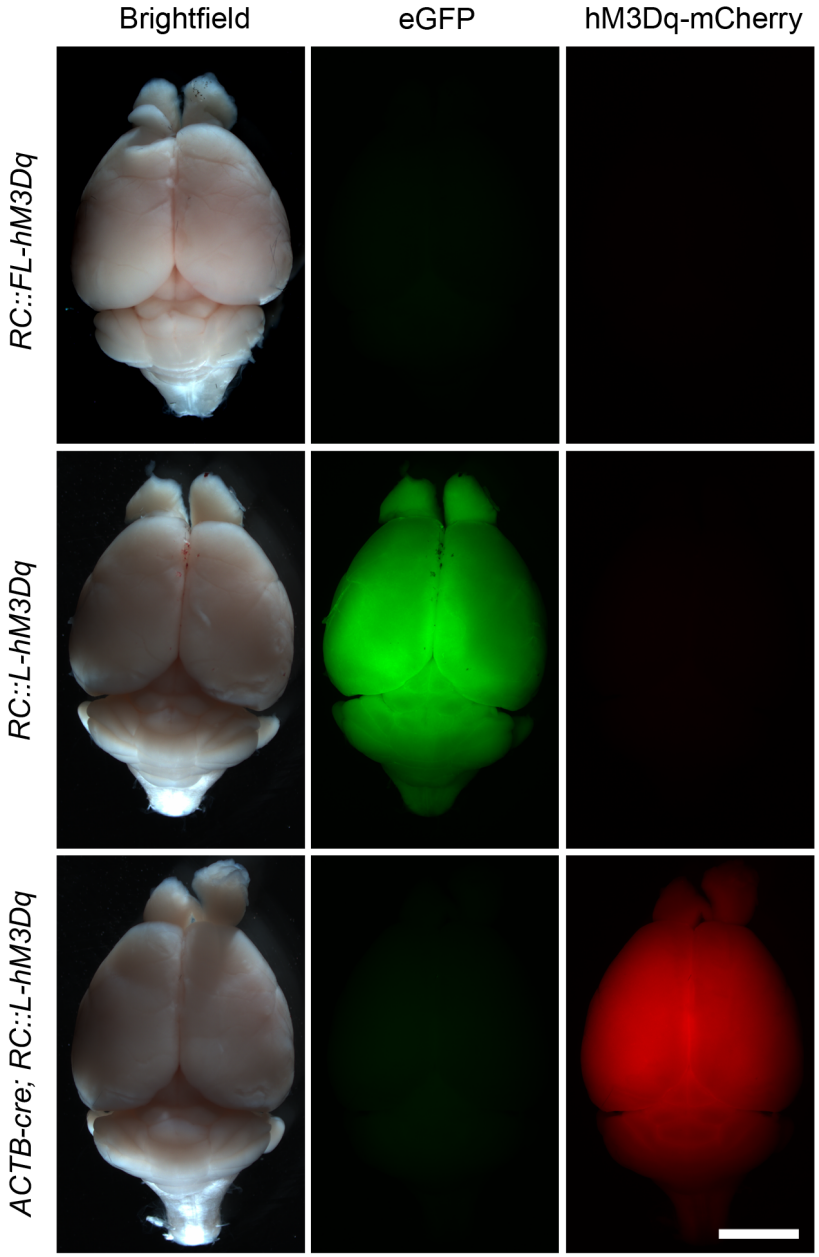

Figure S1. Universal alleles *RC::FL-hM3Dq* and *RC::L-hM3Dq* permit conditional expression of hM3Dq-mCherry and eGFP in the adult brain (Related to Figure 1)
(A) *Top:* In adult *RC::FL-hM3Dq* heterozygous brain, no eGFP or hM3Dq-mCherry is observed in the absence of recombinase. *Middle:* Ubiquitous expression of eGFP, but not hM3Dq-mCherry, is observed in adult *RC::L-hM3Dq* heterozygous brain (equivalent to *RC::FL-hM3Dq* after germline expression of Flp recombinase). *Bottom*: Germline expression of Cre recombinase results in ubiquitous expression of hM3Dq-mCherry in adult *ACTB-cre; RC::L-hM3Dq* brain. Images show native fluorescence. Scale bar: 7 mm.

Figure S2

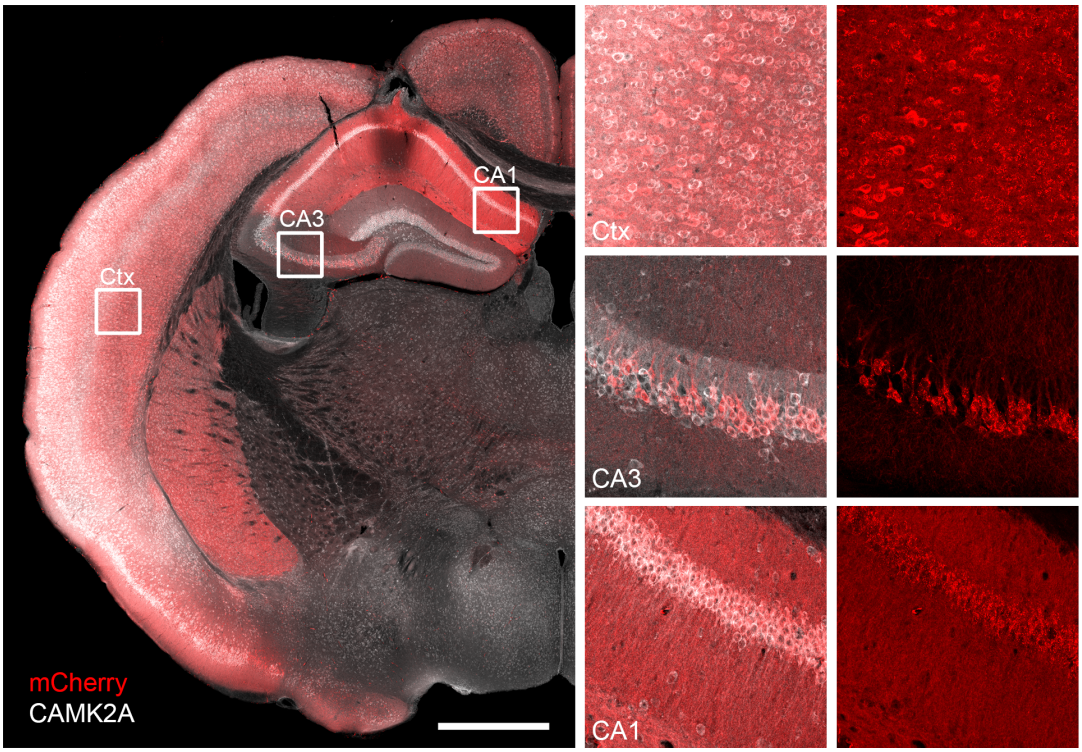

Figure S2: Targeting of hM3Dq-mCherry to CAMK2+ neurons (Related to Figure 3)
Coronal section of a *Camk2a-cre; RC::L-hM3Dq* brain immunolabeled for mCherry (red) and CAMK2A (white). Boxes on the low-magnification image (left) show the location of magnified images. The magnified images show merged mCherry/CAMK2A co-localization (right) or mCherry alone (far right). Consistent with the known expression pattern of the *Camk2a-cre* transgene (Sonner et al., 2005), mCherry is expressed in a large subset of CAMK2A neurons in the cortex (Ctx) and hippocampal CA1, and in scattered cells of other hippocampal regions (CA3 shown). Scale bar: 2000 µm or 165 µm (magnified images).

Figure S3

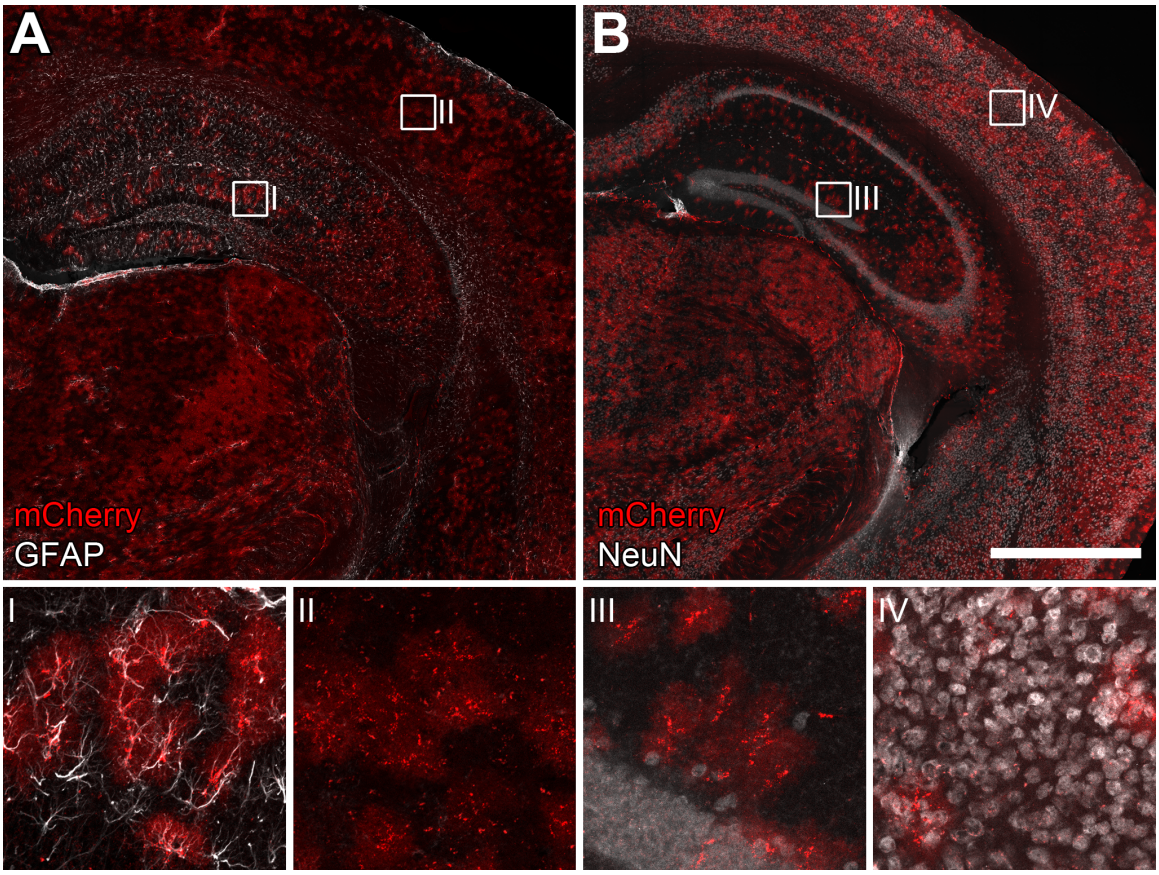

Figure S3: Targeting of hM3Dq-mCherry to GFAP+ glia (Related to Figure 3)
(A) Coronal section of a tamoxifen-treated *GFAP-creERT2; RC::L-hM3Dq* brain immunolabeled for mCherry (red) and the glial marker GFAP (white). Boxes indicate the location of magnified images (I, II). At higher magnification, astrocytes are observed co-labeled with mCherry and GFAP (I). Consistent with known variability in astrocytic GFAP expression and immunolabeling (Sofroniew and Vinters, 2010), mCherry+ glia in some areas (II) are not GFAP immunoreactive,. **(B)** Coronal section of a tamoxifen-treated *GFAP-creERT2; RC::L-hM3Dq* brain immunolabeled for mCherry (red) and the neuronal marker NeuN (white) confirms that mCherry is not expressed in neurons. Boxes indicate the location of magnified images (III, IV). The spatial distribution of mCherry-labeled cells does not match that of NeuN-labeled nuclei, indicating that hM3Dq-mCherry is not expressed in neurons. Scale bar: 1000 µm or 110 µm (magnified images).

Figure S4

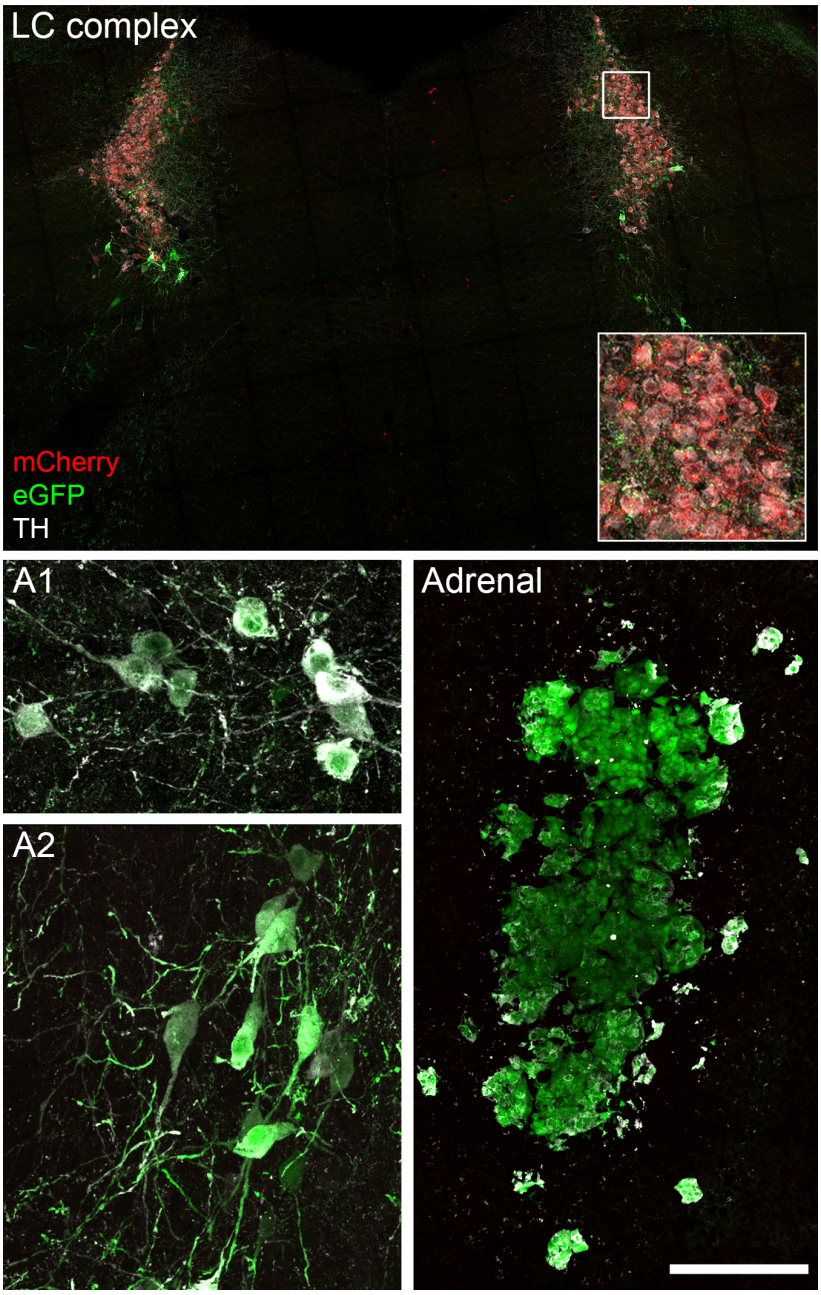

Figure S4: Targeting of hM3Dq-mCherry to the noradrenergic LC complex (Related to Figure 3) Noradrenergic/adrenergic cells of the LC complex, A1, and A2 nuclei in the brainstem and the adrenal medulla of an *En1*^{cre}*; Dbh*^{Flpo}*; RC::FL-hM3Dq* mouse immunolabeled for mCherry (red), eGFP (green), and tyrosine hydroxylase (white). **(Top)** In the LC complex, mCherry is restricted to noradrenergic neurons (TH+) that have a history of both *En1*^{cre} and *Dbh*^{Flpo} expression (Robertson et al., 2013). Noradrenergic neurons in the dorsal subcoeruleus that that originate outside the *En1* expression domain are labeled with eGFP. Non-noradrenergic neurons surrounding the bilateral LC complex are unlabeled. Box indicates the location of magnified inset. **(Bottom)** Noradrenergic/adrenergic cells (TH+) in the A1 and A2 brainstem nuclei and adrenal medulla expressing *Dbh*^{Flpo}, but not *En1*^{cre}, are labeled with eGFP and do not express hM3Dq-mCherry. Scale bar: 500 µm (LC complex), 105 µm (LC complex inset), 72 µm (A1 and A2), or 180 µm (adrenal).

Figure S5

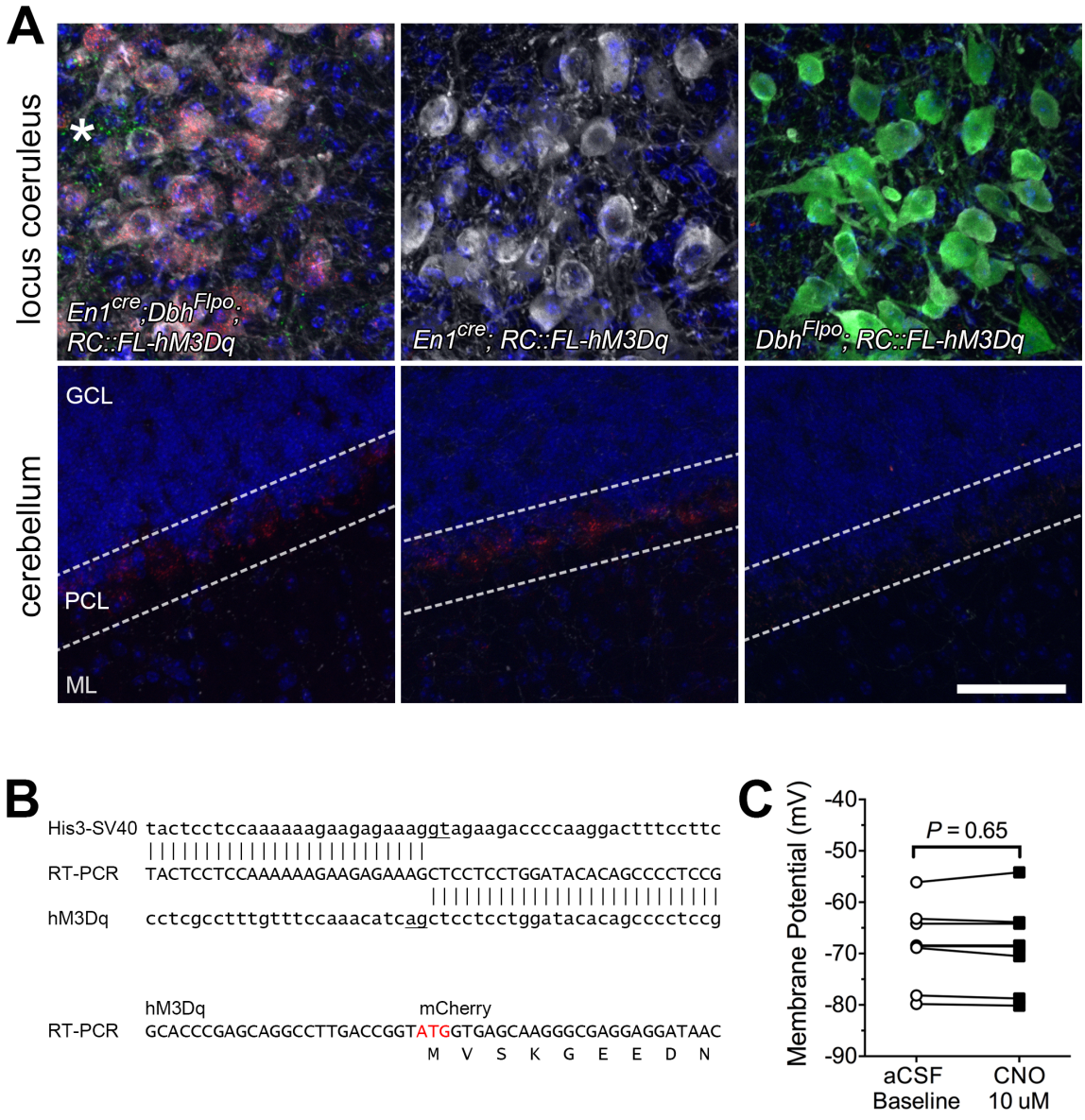

Figure S5. Non-functional, ectopic mCherry fluorescence in Purkinje cells observed following Cre recombination of *RC::FL-hM3Dq* (Related to Figure 4)

(A) Coronal sections of the locus coeruleus and cerebellum stained for DAPI (blue) and immunolabeled for tyrosine hydroxylase (white), mCherry (red), and eGFP (green). *Left:* In *En1^{cre}; Dbh^{Flpo}; RC::FL-hM3Dq* triple heterozygotes, mCherry and eGFP are observed in noradrenergic locus coeruleus neurons and innervating fibers from other noradrenergic nuclei (asterisk), respectively. Purkinje cells express mCherry, but not eGFP. *Middle*: In *En1^{cre}; RC::FL-hM3Dq* double heterozygotes, locus coeruleus neurons are unlabeled, but Purkinje cells express mCherry. *Bottom:* In *Dbh^{Flpo}; RC::FL-hM3Dq* double heterozygotes, locus coeruleus neurons are labeled with eGFP and Purkinje neurons are unlabeled. GCL, granular cell layer; PCL, Purkinje cell layer; ML, molecular layer. Scale bar: 50 µm. **(B)** Sequence from the major RT-PCR product from *En1^{cre}; Dbh^{Flpo}; RC::FL-hM3Dq* cerebellum (uppercase). *Top:* Alignment to His3-SV40 stop cassette and hM3Dq reveals an mRNA splice extending from the middle of the FRT-flanked stop cassette to a cryptic splice acceptor within the hM3Dq cDNA, eliminating the first 77 nucleotides of

hM3Dq. GT and AG dinucleotides of the splice donor and acceptor are underlined. The His3-SV40 sequence and orientation of hM3Dq indicate that the mRNA comes from cells that have expressed Cre but not Flp. *Bottom:* At the site of hM3Dq-mCherry fusion, a start codon (ATG) will permit translation of mCherry without hM3Dq. **(c)** CNO (10 μm) has no effect on membrane potential of mCherry-labeled Purkinje cells (*N*=8 cells from 5 mice) from *En1^{cre}; Dbh^{Flpo}; RC::FL-hM3Dq* triple heterozygotes (Paired *t*-test).

Figure S6

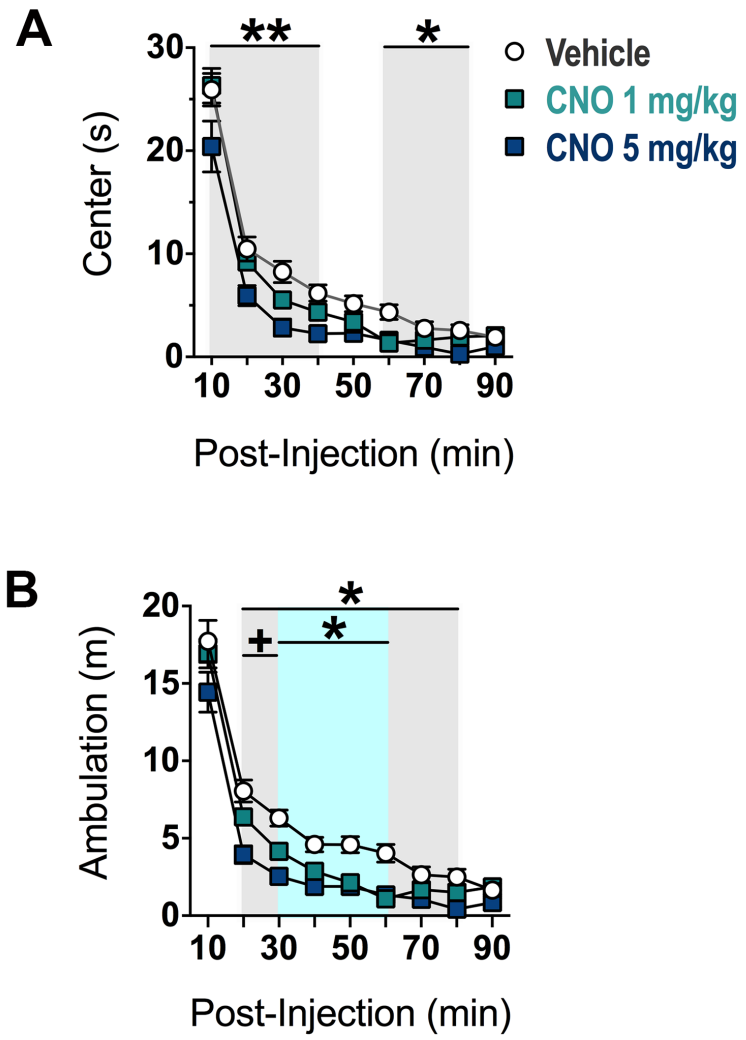

Figure S6: Time course of anxiety-like behavior and locomotor suppression of *En1^{cre}; Dbh^{Flpo}; RC::FL-hM3Dq* mice in the open field test is dependent on the dose of CNO (Related to Figure 5)
(A) The 5-mg/kg dose of CNO reduced center time at 10-40 and 60-80 minutes post-injection compared to vehicle (gray areas on graph). However, center time was not altered by the 1-mg/kg dose of CNO across the experiment. **(B)** The 5-mg/kg dose of CNO significantly reduced ambulation 20-80 minutes post-injection compared to vehicle (gray area on graph). The 1-mg/kg dose of CNO also reduced ambulation 30-60 minutes post-injection (blue area on graph). However, the 5-mg/kg CNO dose produced a greater reduction in ambulation compared to the 1-mg/kg dose only during 20-30 minutes post-injection (gray area denoted by +). Data are ± SEM for vehicle (n=18-20), CNO 1 mg/kg (n=16-18), and CNO 5 mg/kg (n=15) treated *En1^{cre}; Dbh^{Flpo}; RC::FL-hM3Dq* triple heterozygous mice tested in the open field. **p<0.01, *p<0.05 vs. Vehicle (Bonferroni). +p<0.05 vs. CNO 1 mg/kg (Bonferroni).

Figure S7

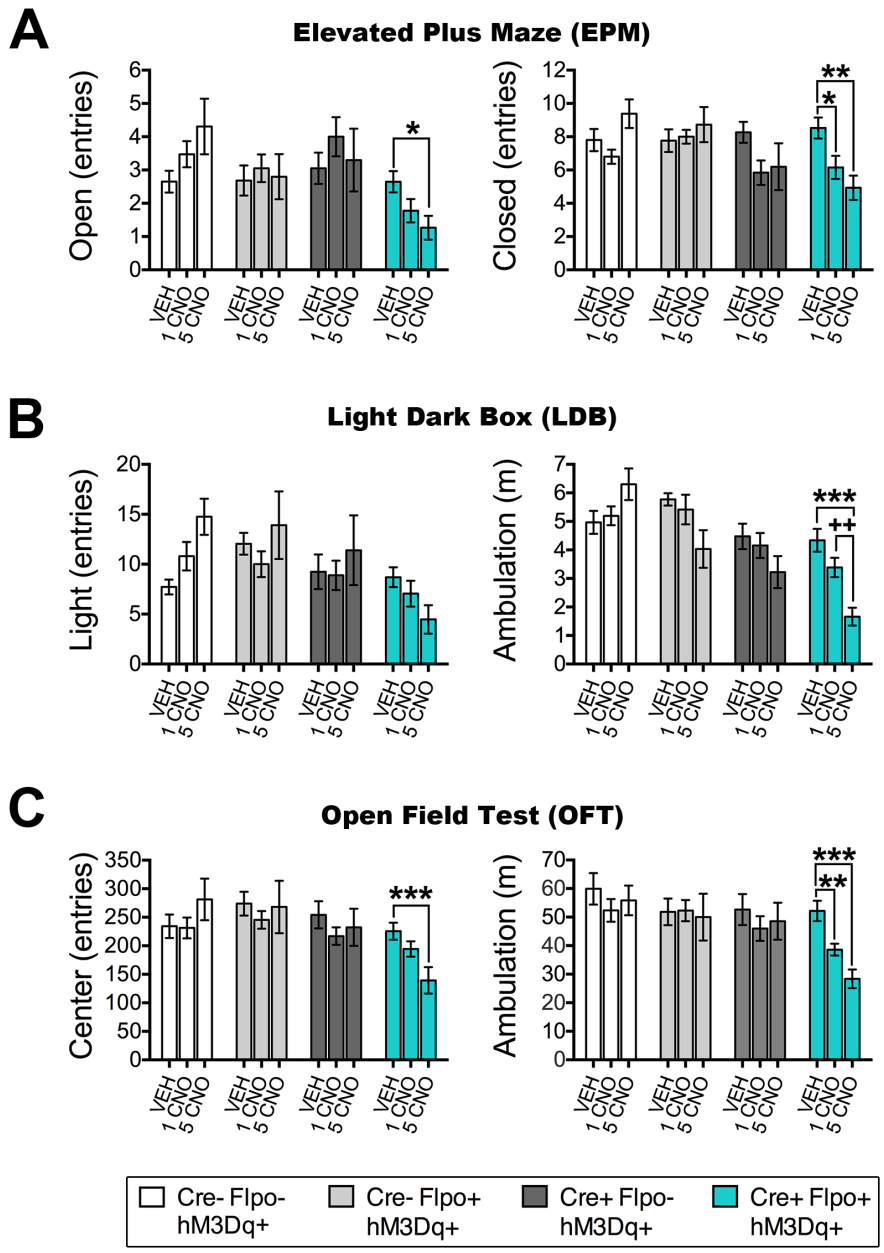

Figure S7. CNO elicits anxiety and hypo-locomotion exclusively in *En1^{cre}; Dbh^{Flpo}; RC::FL-hM3Dq* triple heterozygotes (Related to Figure 5)

(A-C) Behavioral data from elevated plus maze, light-dark box, and open field test. CNO evokes anxiety-like behavior and suppresses locomotion specifically in *En1^{cre}; Dbh^{Flpo}; RC::FL-hM3Dq* mice (Cre+ Flp+). CNO has no effect in littermate controls expressing *RC::FL-hM3Dq* (Cre- Flp), *Dbh^{Flpo}; RC::FL-hM3Dq* (Cre- Flp+) or *En1^{cre}; RC::FL-hM3Dq* (Cre+ Flp-). Data are Mean ± SEM Group sizes are as follows: Vehicle treated Flpo-Cre- (n=17-20), Flpo+Cre- (n=16-21), Flpo-Cre+ (n=17-19), and Flpo+Cre+ (n=17-21); CNO 1-mg/kg treated Flpo-Cre- (n=19-21), Flpo+Cre- (n=19), Flpo-Cre+ (n=18-20), and Flpo+Cre+ (n=16-20); CNO 5-mg/kg treated Flpo-Cre-(n=12-13), Flpo+Cre- (n=10-11), Flpo-Cre+ (n=10-11), and Flpo+Cre+ (n=15). ***p<0.001, **p<0.01, *p<0.05 vs. Vehicle (Bonferroni). $^{++}$p<0.01 vs. CNO 1 mg/kg (Bonferroni).

Table S1: Statistics and sample sizes of behavioral tests (related to Figures 4, Figure S5, Figure S6)

See Excel File.

SUPPLEMENTAL EXPERIMENTAL PROCEDURES

Antibodies

mCherry-expressing cells were detected with either rabbit anti-mCherry primary antibody (1:20,000; Cat.# ab167453, Abcam, Cambridge MA) and Alexa Fluor 568 goat anti-rabbit secondary antibody (1:1000; Cat.# A11036, Thermo Fisher), or rat anti-mCherry primary antibody (1:1000; Cat.# M11217, Thermo Fisher, Waltham, MA) and Alexa Fluor 568 goat anti-rat secondary antibody (1:1000; Cat.# A11077, Thermo Fisher). eGFP-expressing cells were detected with chicken anti-GFP primary antibody (1:10,000; Cat.# ab13970, Abcam) and Alexa Fluor 488 goat anti-chicken secondary antibody (1:1000; Cat.# A11039, Thermo Fisher). Tyrosine hydroxylase-expressing noradrenergic/adrenergic and dopaminergic neurons were detected with rabbit anti-TH (1:1000, Cat.# AB152, Millipore) and Alexa Fluor 633 goat anti-rabbit secondary antibody (1:1000; Cat.# A21071, Thermo Fisher). *Camk2a*-expressing neurons were detected using rabbit anti-CAMK2A (1/250; Cat.# ab131468, Abcam) and Alexa Fluor 633 goat anti-rabbit secondary antibody (1:1000; Cat.# A21071; Thermo Fisher) after antigen retrieval was performed by boiling sections in water for three minutes, followed by incubation in 0.3% Triton X100 for 15 minutes at room temperature. *Gfap*-expressing glia were detected with mouse anti-GFAP primary antibody (1:1000, Cat.# MAB360, Millipore, Billerica, MA) and Alexa Fluor 633 goat anti-mouse secondary antibody (1:1000; Cat.# A21136, Thermo Fisher). NeuN-expressing neurons were detected using mouse anti-NeuN primary antibody (1:1000, Cat.# MAB377, Millipore) and Alexa Fluor 633 goat anti-mouse secondary antibody (1:1000; Cat.# A21136, Thermo Fisher).

Slice Electrophysiology

*Acute Brain Slices***.** For recordings from the LC complex, *En1^{cre}; Dbh^{Flpo}; RC::FL-hM3Dq* and *Dbh^{Flpo}; RC::FL-hM3Dq* mice (N=14, both sexes) were used at 1-3 months of age. For cerebellar Purkinje recordings, *En1^{cre}; Dbh^{Flpo}; RC::FL-hM3Dq* mice (N=8 males) were used at 3-5 months of age. All mice were anesthetized with Pentobarbital and transcardially perfused with chilled (4ºC) and bubbled (95% O_2 and 5% CO_2) high-sucrose, low Na^+ aCSF (sucrose aCSF contained in mM: 182 sucrose, 20 NaCl, 0.5 KCl, 1 $MgCl_2$-$6H_20$, 1.2 NaH_2PO_4-H_20, 26 $NaHCO_3$, 10 glucose). Mice were quickly decapitated and brains were removed and placed in sucrose aCSF. Coronal slices (250 µm) containing the LC complex and/or cerebellum were cut on a VT1200S vibratome (Leica Biosystems, Buffalo Grove, IL) in sucrose aCSF, and incubated for at least 30 min at 28-30ºC in oxygenated aCSF (aCSF that contained in mM: 124 NaCl, 4 KCl, 1.2 $MgSO_4$-$7H_20$, 2 $CaCl_2$-$2H_20$,1 NaH_2PO_4-H_20, 13 $NaHCO_3$, 5 glucose).

General Recording Methods. Slices were transferred to a recording chamber (RC-26G, Warner Instruments, Hamden, CT) and allowed to rest for an additional 30 min while continuously perfused with heated (32ºC), oxygenated aCSF (CL-100 temperature controller and LCS-1 cooling system, Warner Instruments) at 2 mL/min (Peri-Star Pro peristaltic pump, World Precision Instruments, Sarasota, FL). Data were collected at 10 kHz using an EPC 800 amplifier (HEKA Elektronik, Lambrecht, Germany) equipped with DigiData 132x digitizer and pClamp 10.4 software (Molecular Devices, Sunnyvale CA) on a Dell Precision T3610 computer. Patch electrodes were fashioned using borosilicate glass capillary tubing (1.5 mm o.d., 1.12 mm i.d., TW150F-4, World Precision Instruments) pulled by a P97 Flaming Brown microelectrode puller (Sutter, Novato, CA). Neurons were visualized at 40x using a Zeiss Axio Examiner microscope equipped with Axiocam 503 camera (Carl Zeiss Microscopy, Thornwood, NY) and PhotoFluor II light source (89 North, Burlington, VT).

Whole-Cell Recording. Recordings were made from eGFP+ and hM3Dq-mCherry+ neurons of the LC complex, and mCherry+ cerebellar Purkinje cells in current clamp mode. After 5-10 min to allow the baseline to stabilize, membrane potential was recorded in LC neurons before and during bath application of CNO (10 µM, NIDA Drug Supply Program) and then during and after bath application of the positive-control NMDA (50 µM, Sigma, St. Louis, MI). Methods were similar for recordings from mCherry+ cerebellar Purkinje cells, except that membrane potential was recorded before, during, and after bath application of CNO (10 µM). Tip resistance was 3-5 MΩ when electrodes were filled with intracellular solution containing (mM): 135 K Gluc, 5 NaCl, 2 $MgCl_2$-$6H_20$, 10 HEPES, 0.6 EGTA, 4 Na_2ATP, 0.4 Na_2GTP. AlexaFluor 350 dye (Thermo Fisher Scientific) was added to the intracellular solution. Liquid

junction potential was +13 mV and membrane potential was adjusted and reported accordingly.

Cell-Attached Recording. Loose seal recordings (<20 MΩ) were made from hM3Dq-mCherry+ neurons of the LC complex in voltage clamp mode. Traces were monitored for 5-10 minutes to determine whether baseline-firing rate was stable. During this time, a voltage command was applied to shift the baseline to 0 pA to negate current due to a change in the junction potential. Next, firing rate was continuously recorded before, during, and after bath application of CNO (10 μM, NIDA Drug Supply Program). Tip resistance of the recording electrode was 1-3 MΩ when filled with aCSF.

Data Analysis for Slice Electrophysiology. All analyses were performed using ClampFit 10.4 (Molecular Devices). Voltage traces were low-pass filtered at 3 Hz using a Gaussian function, and only recordings with an access resistance of <30 MΩ were included for analysis (Niculescu et al., 2013). Membrane potential was averaged across a recording period of 1 minute (Purkinje recordings) or 2 minutes (LC recordings) within each drug application phase. Each period was selected during the center of each drug phase to avoid inclusion of potential artifact from transition between drugs. LC neurons with resting membrane potentials > -39 mV were excluded to avoid the possibility of including unhealthy cells (e.g., cells damaged during slice preparation) (van den Pol et al., 2002). Only one hM3Dq+ neuron, exhibiting a slight hyperpolarization (by -1.62 mV) during CNO application, was excluded from analysis because it's membrane potential met the outlier criteria (3 SD±Mean). Independent *t*-tests were used to assess whether membrane potential was altered by CNO or recording parameters (TTX vs. TTX+Nimodipine). Two-way ANOVA with Bonferroni follow-up tests were used to determine whether CNO altered membrane potential in a manner dependent on mouse genotype. Current traces were high-pass filtered at 1 Hz, and only LC recordings with a seal resistance of 5-20 MΩ were included for analysis (Nunemaker et al., 2003). Firing rate was averaged across 2-minute periods of recording within each drug application phase. Paired samples t-test was used to determine whether firing rate was altered by CNO.

Drugs for In Vitro Electrophysiology. All stock solutions were diluted in aCSF to final concentration. Stocks of CNO and nimodipine were made in DMSO, and TTX and NMDA were made in ddH_2O. The final volume of DMSO or ddH_2O did not exceed 0.24% or 0.01%.

Anxiety-like Behavior

General Procedure for the Anxiety Test Battery. Male and female (N=210 mice weighing 15-37 g) *En1^{cre}; Dbh^{Flpo}; RC::FL-hM3Dq* and littermate controls were group housed, with *ad libitum* food and water. Mice were housed under a 12:12 light:dark cycle, and were tested in the anxiety test battery during lights ON. Mice were randomly assigned at approximately 2-6 months of age to receive two intraperitoneal (i.p.) injections of vehicle (0.6% DMSO in saline) or clozapine N-oxide (1 or 5 mg/kg.) prior to testing. The first administration of the assigned drug was given immediately before placement in the open field. The second administration was given 2-3 days later, approximately 15 min before the light dark box (LDB) test. Directly after the LDB, Mice were tested in the elevated plus maze (EPM). All injections were administered at 0.1 mL/10 g using drug prepared fresh daily. The experimenter was blind to the assigned drug and genotype for all experiments. Equipment was cleaned between tests using Accel wipes (0.5% Hydrogen Peroxide, AHP Technologies).

Open Field Test (OFT). Mice were placed in the center of an activity monitor box (ENV-510; 27 x 27 x 20 cm, Med Associates) that was enclosed in a sound-attenuated cubicle. For 90 minutes, mice were allowed to freely explore the non-illuminated apparatus (0 lux). Mouse position and movement was tracked by infrared beam breaks measured every 50 milliseconds within the center (14.3 x 14.3 cm) and remaining periphery of the apparatus (SOF-810 version 7, default settings). Ambulation was detected when movement triggered three beam breaks and measured thereafter as distance traveled in continuous (longer than 500 ms) movement outside a 2 by 2 area of x–y beams. Center time and entries are reported as the standard measures of anxiety-like behavior. We also verified that manipulations that changed center exploration had an opposite effect on periphery exploration. Ambulatory distance is reported as an index of locomotion.

Light Dark Box (LDB). The LDB apparatus was divided into a dark (ENV-511; 13.5 x 27 cm) and light side (13.5 x 25 cm). Mice were placed in the light side of the apparatus (ENV-510, Med Associates), and allowed to freely explore both dark (0 lux illumination) and light compartments (~950 lux) for 10 min while behavior was detected automatically by infrared beam breaks (see OFT section for details). Time spent and entries into the light compartment are reported as standard measures of anxiety-like behavior during the last 5 min of the LDB test. This time window corresponds to 20-25 min post-injection, and was selected for analysis to illustrate the anxiogenic effect elicited by CNO, which would otherwise go undetected if data were reported across the entire test duration. Manipulations that changed light chamber exploration were confirmed to have an opposite effect on dark chamber exploration. Ambulatory distance during the last 5 min of the LDB test is reported as the locomotor index.

Elevated Plus Maze (EPM). Directly after LDB testing, mice were placed on a '+' shaped maze standing 20" from floor with a pair of open (11 x 2 inch) and closed arms (11 x 2 x 5 inch) that meet at a central platform (2 x 2 inch). The maze was illuminated at 300 lux. Mice were placed on the center zone facing an open arm and allowed to freely explore for 5 min. Exploration was recorded and analyzed from video by an experimenter blind to genotype and drug treatment. Entrance of all four paws was required to count as a new arm entry (Sciolino et al., 2015). Open arm time and entries are reported as the primary measure of anxiety-like behavior. In addition, manipulations that changed open arm time were also verified to have an opposite effect on closed arm time. Closed arm entries are reported as a proxy of locomotor behavior.

Data Analysis for Anxiety-Related Behavior. To avoid a type II statistical error, Tukey's strategy (1.5 IQR above or below the 25^{th} or 75^{th} percentile) was used for detection and removal of extreme outliers. This conservative strategy identified outliers that occurred infrequently in the dataset (0.03 of values), and importantly similar overall results were obtained regardless if outliers were included or excluded. One-way ANOVAs were used to determine whether CNO altered behavior in *En1^{cre}; Dbh^{Flpo}; RC::FL-hM3Dq* mice. Two-way ANOVAs were used to determine whether the effect of CNO was dependent on mouse genotype. Bonferroni post-hoc tests were conducted when appropriate.

In Vivo Electrophysiology

Animals and Surgery. Multielectrode bundles were surgically implanted in 10 mice with the following genotypes: *Camk2a-cre; RC::L-hM3Dq* (n=4), *Camk2a-cre* (n=3), and *RC::L-hM3Dq* (n=3). Mice, at least 8 weeks of age, were anesthetized with ketamine (100 mg/kg) and xylazine (7 mg/kg) and placed in a stereotax. Four metal anchors and a ground screw were secured in the cranium. A craniotomy was made over the left dorsal hippocampus, and a bundle of 10 wires in medical grade tubing were implanted in the hippocampus using the following stereotaxic coordinates (mm): -2.06 anteroposterior, 2.1 mediolateral, 2.1 dorsoventral from bregma (Paxinos and Franks, 2013). Implanted electrodes were secured to the skull with dental acrylic, and mice were treated with buprenorphine (0.05 mg/kg) to alleviate post-surgical pain.

In Vivo Electrophysiology Recordings. Electrodes were constructed from 44µm polyimide-coated stainless steel wires (Sandvic Materials Technology, Sandviken, Sweden) that connected to a printed circuit board (San Francisco Circuits, San Francisco, CA) and miniature connector (Omnetics Connector Corporation, Minneapolis, MN). Electrode tips were cut to length on the day of surgery. Recordings of neural activity were transmitted via a wireless 32-channel 10x gain headstage (Triangle BioSystems International, Durham, NC) acquired using the Cerebus acquisition system (Blackrock Microsystems, Salt Lake City, UT). Continuous local field potential (LFP) data were band-pass filtered at 0.3–500 Hz and stored at 1,000 Hz. All recordings were referenced to the ground wire connected to a ground screw.

A week after recovery from surgery, recordings were made before, during and after administration of vehicle or CNO. We adopted the dosing regimen used to characterize the original hM3Dq transgene to directly compare our data to prior results (Alexander et al., 2009). Vehicle (1.5% DMSO in saline) and the following escalating doses of CNO were administered with 2-3 days between treatments: 0.03 mg/kg, 0.1 mg/kg, 0.3 mg/kg, 0.5 mg/kg, 1 mg/kg, 5 mg/kg and 10 mg/kg. Electrophysiological recordings were not

obtained upon administration of 0.03 or 0.1 mg/kg CNO, but recordings were made upon all other administrations. For all recordings, a baseline period of at least 30 minutes was included before administration of either vehicle or CNO, and recordings were made for 1.5-2 hours following injection. Animals were in a clear plexiglass chamber (20" x 20") during recordings. The experimenter was blind to genotype for all experiments.

Data Analysis for In Vivo Electrophysiology. Analysis of local field potentials (LFPs) were performed using Matlab (version R2014a, MathWorks, Inc., Natick, MA) with Chronux software (http://chronux.org/) (Mitra and Bokil, 2007). LFPs were monitored for the presence of ictal activity following CNO administration. For power spectral analyses of LFPs, spectrograms were first generated to visualize changes in LFP frequency following vehicle or CNO administration. Subsequent power spectral density analyses were used to measure changes in peak gamma (50-80 Hz) power in successive 5-min blocks of LFP data. Peak gamma powers following injection were normalized to pre-injection gamma power, which was calculated by averaging the peak gamma power over the five time bins between 0 and 25 minutes. The 25-30 min time bin was not included in gamma power analysis because mice were handled and injected during this time. Peak gamma powers following vehicle or CNO administration were compared for hM3Dq-expressing and littermate control mice for all treatments using a one- or two-way ANOVA with Bonferroni follow-up tests. Littermate controls heterozygous either for *RC::L-hM3Dq* or *Camk2a-cre* showed no differences in peak gamma power, and thus were combined for analyses.

Body Temperature

Animals and Procedures. Tamoxifen-treated *GFAP-creErt2; RC::L-hM3Dq* double heterozygous mice and littermate controls (N=48, male and female) were tested at 3-5 months of age. Mice (18-29 g) were group housed, with *ad libitum* food and water on a 12:12 light:dark cycle. Mice were restrained to measure baseline body temperature using a rectal probe. Directly after, mice were injected with either vehicle (0.6% DMSO in saline) or CNO (1 or 5 mg/kg, i.p.) and temperature was repeatedly measured every 10 minutes for 90 min post-injection. All mice were tested twice with at least 5 days of recovery between the two tests. A heating pad was made available post-testing to mice exhibiting low-body temperature. Injections were administered at 0.1 mL/10 g using drug prepared fresh daily. The experimenter was blind to drug treatment and genotype for all experiments.

Data Analysis for Body Temperature. Group differences were assessed by one- or two-way ANOVAs followed by Bonferroni multiple comparisons. The results obtained from two repeated vehicle-testing trials were averaged for each subject.

SUPPLEMENTAL REFERENCES

Alexander, G.M., Rogan, S.C., Abbas, A.I., Armbruster, B.N., Pei, Y., Allen, J.A., Nonneman, R.J., Hartmann, J., Moy, S.S., Nicolelis, M.A.*, et al.* (2009). Remote control of neuronal activity in transgenic mice expressing evolved G protein-coupled receptors. Neuron *63*, 27-39.

Mitra, P., and Bokil, H. (2007). Observed Brain Dynamics, 1 edn (USA: Oxford University Press).

Niculescu, D., Hirdes, W., Hornig, S., Pongs, O., and Schwarz, J.R. (2013). Erg potassium currents of neonatal mouse Purkinje cells exhibit fast gating kinetics and are inhibited by mGluR1 activation. J. Neurosci. *33*, 16729-16740.

Nunemaker, C.S., DeFazio, R.A., and Moenter, S.M. (2003). A targeted extracellular approach for recording long-term firing patterns of excitable cells: a practical guide. Biol Proced Online *5*, 53-62.

Paxinos, G., and Franks, K.B.J. (2013). The mouse brain in sterotaxic coordinates (San Diego: Academic Press).

Sciolino, N.R., Smith, J.M., Stranahan, A.M., Freeman, K.G., Edwards, G.L., Weinshenker, D., and Holmes, P.V. (2015). Galanin mediates features of neural and behavioral stress resilience afforded by exercise. Neuropharmacology *89*, 255-264.

Sofroniew, M.V., and Vinters, H.V. (2010). Astrocytes: biology and pathology. Acta Neuropathol. *119*, 7-35.

Sonner, J.M., Cascio, M., Xing, Y., Fanselow, M.S., Kralic, J.E., Morrow, A.L., Korpi, E.R., Hardy, S., Sloat, B., Eger, E.I., 2nd, and Homanics, G.E. (2005). Alpha 1 subunit-containing GABA type A receptors in forebrain contribute to the effect of inhaled anesthetics on conditioned fear. Mol. Pharmacol. *68*, 61-68.

van den Pol, A.N., Ghosh, P.K., Liu, R.J., Li, Y., Aghajanian, G.K., and Gao, X.B. (2002). Hypocretin (orexin) enhances neuron activity and cell synchrony in developing mouse GFP-expressing locus coeruleus. J. Physiol. *541*, 169-185.